

# Calibration of the High Momentum Spectrometer Drift Chambers

Carlos Yero  
April 26, 2017

**Abstract**—The calibration procedure for *horizontal* drift chambers in the High Momentum Spectrometer (HMS) is outlined. The main objective of this calibration was to produce a time-to-distance map in order to determine the position of particle tracks from the measured drift times. Using the calibration results, a brief study about drift velocities was also done in which it was found that they vary from  $\sim 40\text{--}55\mu\text{m/ns}$  in regions of approximately uniform electric fields. Finally, efficiency and residuals on both chambers was investigated and determined each plane to be better than 94% efficient, with spatial resolutions better than  $420\mu\text{m}$ .

## I. INTRODUCTION

AS part of the plan to commission the Super HMS (SHMS) at Hall C - Jefferson Lab, the HMS also needs to be operational for coincidence experiments. The drift chambers are an essential element of the spectrometer as they are needed for particle tracking and reconstruction. (See Figure 1) One of the drift chambers in the HMS had 97 sense wires and 1 field wire damaged from years of exposure to radiation since it was first installed in the detector stack in 1995 [2]. The wires were replaced on Fall 2016 and both chambers were verified to be operational by performing several cosmic<sup>1</sup> tests. On March 2017, as part of the Key Performance Parameters (KPP) needed to be satisfy by Hall C to demonstrate that the SHMS was in operating conditions, data was taken with actual beam in the Hall. Data with the HMS was also taken and used to calibrate the drift chambers.

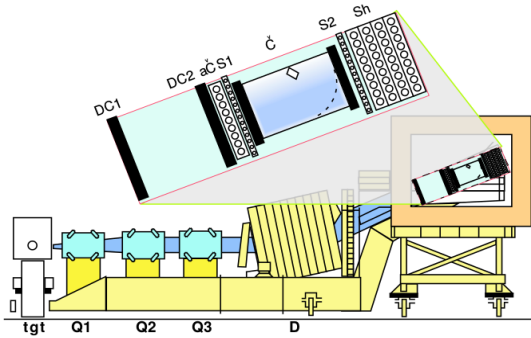


Fig. 1: HMS carriage showing the magnet elements (Quadrupoles ( $Q_i$ ), Dipole (D)). The detector elements are after the  $25^\circ$  bend, where DC1 and DC2 denotes the drift chamber packages 1 and 2.

## II. PRINCIPLE OF OPERATION

Each drift chamber consists of 6 planes (X, Y, U, V, Y', X'), where the X(X') are orthogonal to Y(Y') planes, and U and V are tilted  $15^\circ$  relative to X(X'). (See Figure 2) Each

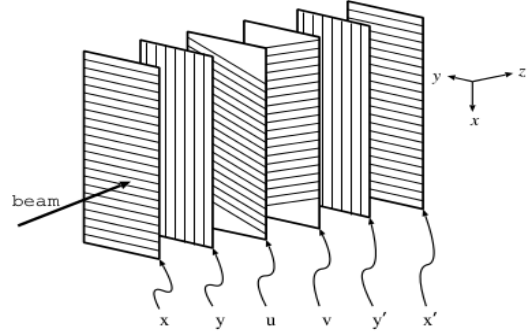


Fig. 2: Schematic of drift chamber planes. Figure courtesy of C. Armstrong.

plane consists of an array of alternating field and sense wires<sup>2</sup> (0.5 cm apart) surrounded by two arrays of field wires so that each sense wire is surrounded by 8 field wires, forming a cell. (See Figure 3) The field wires are kept at a negative potential

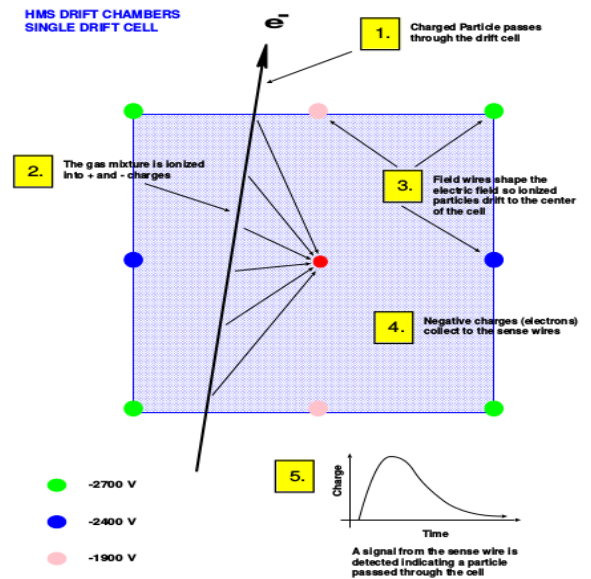


Fig. 3: Schematics of a single cell in a drift chamber plane. Figure courtesy of G. Niculescu and D. Abbot.

while the sense wires are grounded (0 V). Due to the potential difference between the field and sense wires, an electric field is established which causes free electrons from ionized gas atoms and molecules of the gas mixture<sup>3</sup> to drift towards the sense wires producing a measurable signal. The sense wire signals are pre-amplified and read by 16-channel input discriminators which produce logic signals that lead into Time-to-Digital Converters (TDCs) by twisted pair ribbon cables[1]. The TDCs

<sup>2</sup>Total sense wires per plane: X,X'-113, Y,Y'-52, U,V-107

<sup>3</sup>Drift chambers are filled with a gas mixture mainly to make the ions drift velocity as uniform as possible.

<sup>1</sup>Cosmic tests refers to the detection of cosmic rays or highly energetic particles (mainly protons) originating mostly outside of the solar system.

registers the total travel time of the signal since it was created by the passing particle. This time is compared to the surveyed time it would have taken the signal to propagate across the sense wire, through the ribbon cable into the TDC if the particle would have passed through the sense wire. The time difference is known as the *drift time*, or the time it takes the free electrons to drift towards the sense wire. Mathematically, the drift time can be expressed as,

$$t_D = (t_{meas.} - t_{REF}) - \underbrace{[(t_{wire} + t_{cable}) - t_{REF}]}_{t'} \quad (1)$$

where  $t_{meas.}$  is the measured time by the TDC, and  $t'$  is the time it takes the signal to propagate across the sense wire and through the cable into the TDC if the track would have passed through the sense wire. These times are measured relative to a reference time<sup>4</sup>  $t_{REF}$ , used by the TDCs in Common Stop Mode (analogous to a stopwatch).

For a charged particle that traverses the drift chamber, only certain sense wires will fire. If a wire, say in the X-plane fires, one does not know if the particle passed the left or right side of the chamber relative to the wire. By including the X'-plane, the left-right ambiguity is removed since the particle will fire a wire in X' which allows one to determine the x-coordinate of the track. Similarly, for the Y (Y') planes, the y-coordinate of the track is determined and the U (V) planes provide angle information about the track.

A coarse track reconstruction can be done with only the knowledge of the wires that fire from a physics event. Knowing the associated drift times of the wires that were hit, however, allows for a more precise track reconstruction, as the drift time can be converted to a drift distance from the determination of time to distance maps from calibration. The drift distances can be added as fine corrections to the coarse track reconstruction.

### III. CALIBRATION PROCEDURE

For many events illuminating all cells in any give plane, one obtains a drift time distribution for each sense wire which are then averaged over the entire plane to form a drift time distribution per plane.(see Figure 4)

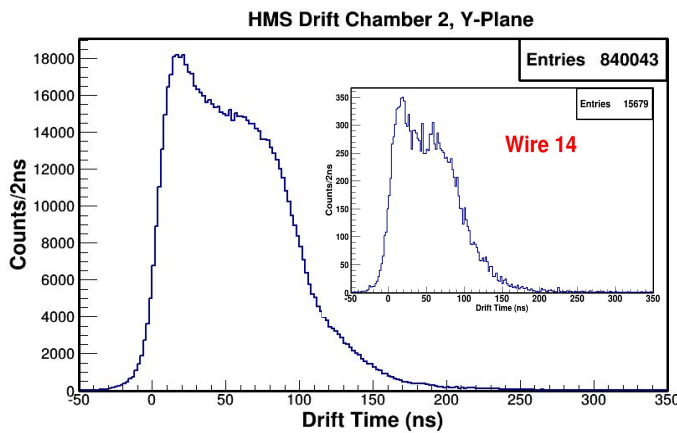


Fig. 4: Averaged and single wire drift time spectra in the Y-plane of drift chamber 2.

<sup>4</sup>Reference time (trigger) is defined based on certain conditions that a signal must pass for it to be considered as a physical event. In the HMS in particular, it was defined as a 3/4 hodoscope plane coincidence - or the signal must have been detected in at least 3/4 hodoscope planes within a time window for it to be considered a true event (or trigger).

Associated with each drift time spectra is a quantity called “ $t_0$ ”. The “ $t_0$ ” corresponds to the location in the histogram where the ionized particle comes in contact with the wire. If its value is anything other than zero nanoseconds (0 ns), it is interpreted as the value by which the drift time must be shifted in order to align the “ $t_0$ ” with 0 ns. All subsequent times in each drift time spectra are measured relative to this time.

The “ $t_0$ ” for each plane is determined by calculating the “ $t_0$ ” for individual wires in each plane and taking a weighted average. The “ $t_0$ ” for individual sense wires is determined by a linear fit of the wire drift time spectra at around 20% of the peak  $\pm \Delta t$  for each sense wire, where  $\Delta t$  is the fit range. The linear fit is then extrapolated to the horizontal axis (drift time), and this extrapolated value is defined as “ $t_0$ ”. (See Figure 5)

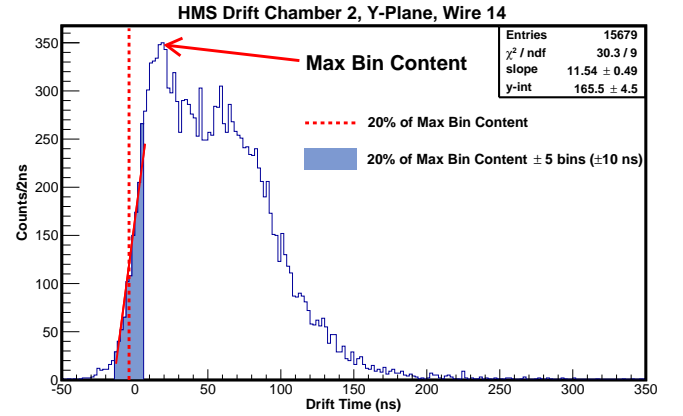


Fig. 5: Linear fit to drift time of sense wire 14 in the Y-plane of the second drift chamber. The fit is extrapolated to the x-axis to determine “ $t_0$ ”.

Less than a percent of the total wires in the second drift chamber were found dead<sup>5</sup>, while other wires had low statistics due to the biased direction of the particles entering the detector stack. This effect can be observed from the wire hitmaps in Figure 6. The central wire from the Y-plane has the highest

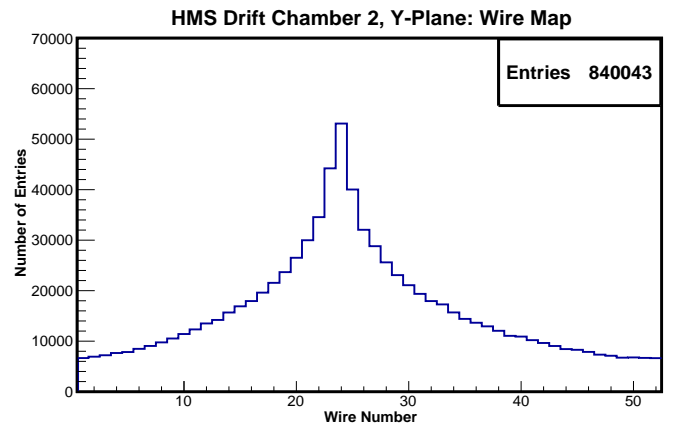


Fig. 6: Wire map showing the number of entries (hits from physics events) received by each sense wire in Y-plane of the second drift chamber.

number of entries and fall exponentially for wires further from the center. This effect is due to the spectrometer magnets focusing the particles that enter the detector stack towards

<sup>5</sup>Wires with no registered hits, except noise from the electronics, are defined as dead.

the center (focal plane) of the two chambers. The calibration run taken had enough statistics, that even at the edge, wires had sufficient events for a linear fit to be made. Dead wires found in other planes were excluded from the fit, as they would have been outliers in the data, causing a shift in the weighted average. The weighted average for the Y-plane of drift chamber 2 is shown in Figure 7.

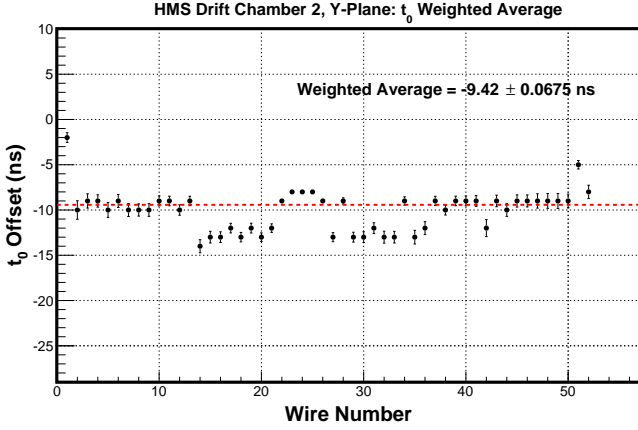


Fig. 7: Weighted average of the “ $t_0$ ” offset for all wires in the Y-plane of drift chamber 2.

The weighted average over all wires is assigned as the “ $t_0$ ” of the plane. When this procedure is done for all planes in both chambers, the drift times should be aligned at  $t_0=0$  ns. (See Figure 8)

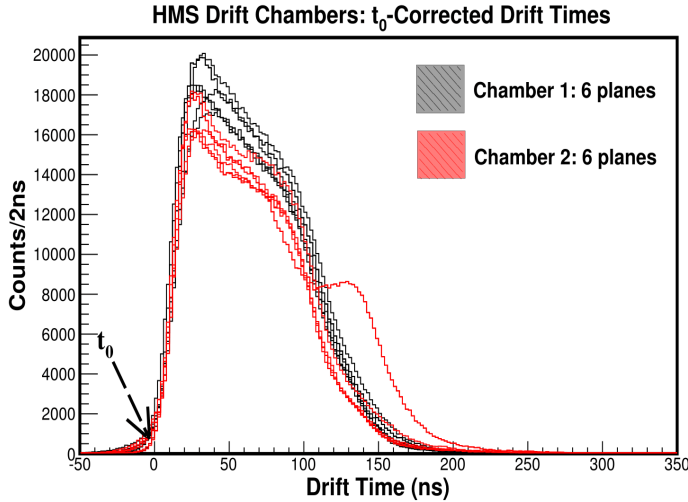


Fig. 8: Corrected drift time spectra for all planes in both drift chambers.

To determine the drift distances from drift time spectra, it is assumed that the drift distance is uniformly distributed across the cell. This assumption is based on the fact that a cell is uniformly illuminated with particles, and the ions have an approximately uniform drift velocity which implies there should be no preferred drift distance for any ionized charge. Mathematically, the drift distance is calculated as follows,

$$d_{drift}(\tau = T) = \frac{\Delta}{2} \frac{\int_{t_0}^{T \leq t_{max}} F(\tau) d\tau}{\int_{t_0}^{t_{max}} F(\tau) d\tau} \quad (2)$$

where  $\Delta$  is the cell width and  $F(\tau)$  is the drift time distribution integrated from  $t_0 = 0$  ns to some arbitrary time  $T < t_{max}$  where  $t_{max}$  is maximum drift time within a cell.

The normalization constant in front of the integral is the maximum drift distance (0.5 cm). In the limiting cases of Eq.2, the drift distance becomes

$$d_{drift} = \begin{cases} 0 \text{ cm}, & \tau = 0 \text{ ns} \\ 0.5 \text{ cm}, & \tau = t_{max} \end{cases} \quad (3)$$

which is the expected drift distance at the sense wire ( $\tau = 0$ ns) and at the edges of the cell ( $\tau = t_{max}$ ).

Due to the finite resolution of the TDCs and other factors involved, the drift times are not determined to infinite precision and the integrals in Eq.2 become a sum over a finite bin width,

$$\int_{\tau} F(\tau) d\tau \rightarrow \sum_{bin(\tau)} \underbrace{F(\tau)}_{binContent} \cdot \underbrace{\Delta\tau}_{binWidth}$$

Re-writing the ratio of integrals Eq.2 in terms of the finite sums, one obtains

$$\frac{\sum_{bin(t_0)}^{bin(t_0+T)} F(\tau) \Delta\tau}{\sum_{bin(t_0)}^{bin(t_0+t_{max})} F(\tau) \Delta\tau} \rightarrow \frac{1}{N_{tot.}} \sum_{bin(t_0)}^{bin(t_0+T)} F(\tau) \quad (4)$$

The ratio in Eq.4 are the lookup values used to convert drift time to distance for an arbitrary drift time. The numerator represents the sum of all bin contents up to a drift time  $T$ , and the denominator represents the sum over the bin contents of all drift times up to  $t_{max}$ , in a given plane. The bin width,  $\Delta\tau$ , is a constant (2 ns) during the sum, therefore it is cancelled, which simplifies the equation as a ratio of the sum of bin contents (up to some drift time) and the sum over all bin contents (up to a maximum,  $t_{max}$ ),  $N_{tot.}$

The results of this calibration are per plane look-up tables that map any given drift time to a drift distance in that plane. The drift distance for the Y-plane of drift chamber 2 is shown in Figure 9. As expected, the drift distances for all planes are

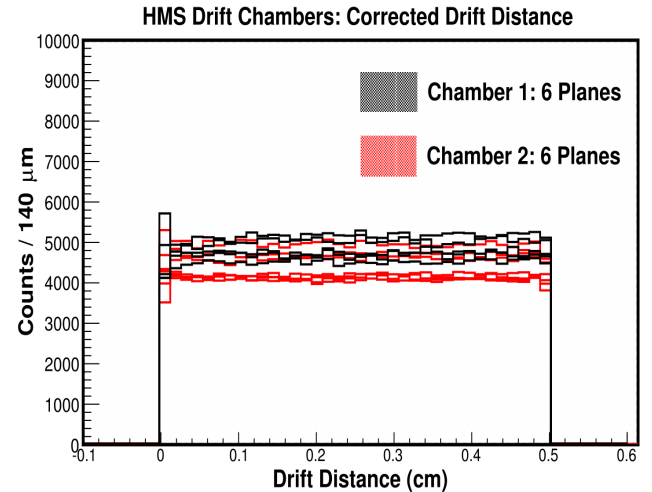


Fig. 9: Corrected drift distance spectra for all planes in both drift chambers.

uniformly distributed across the cell width. A minor problem encountered during the calibration procedure was that for some of the calculated drift distances, there was either a large and small number of counts at the edges (0 or 0.5 cm) whereas in the central region ( $\sim 0.1-0.3$ cm), the counts were uniformly distributed. (See Figure 10)

The weighted  $t_0$ 's determined from calibration had to be

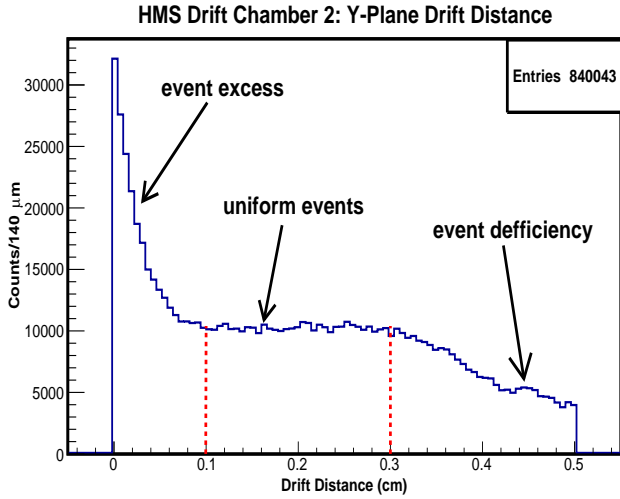


Fig. 10: Uncorrected drift distance spectrum.

manually offset in order to correct for events accumulating at the edges. This is due to a significant variation ( $\sim 5$ -10 ns) in the  $t_0$ 's for groups of wires in a plane, which affects the weighted average for that plane. To overcome this difficulty, the  $t_0$ -correction must be applied to individual sense wires rather than taking a weighted average. The procedure to include individual wire  $t_0$ -offsets is currently in progress.

#### IV. DRIFT VELOCITY CALCULATION

Drift velocities of free electrons are sensitive to the gas mixture used in the chamber as well as the high voltage applied to field wires, as they govern the shape of the electric field that will cause ions to drift. A typical graph of drift velocities as a function of field strength for various Argon/Ethane mixtures. mixtures is shown in Figure 11.

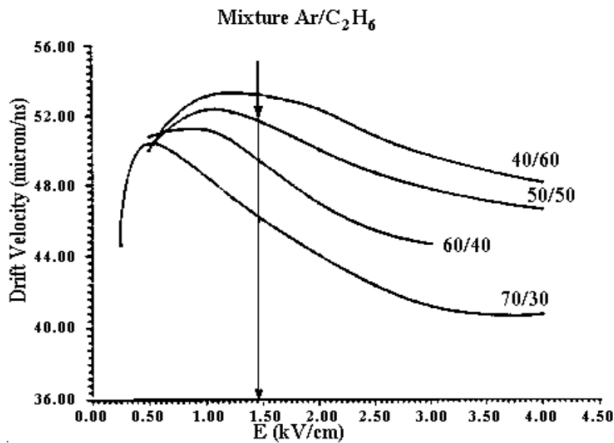


Fig. 11: Drift velocity variation with electric field. Figure courtesy of PHOENIX at Brookhaven National Lab (BNL).

During the calibration run, the HMS drift chambers operated at a 50:50 mixture by volume of Argon/Ethane. The drift velocities were determined by taking the ratio of drift distance to drift time per plane. The correlation shows a linear relationship between distance and time indicating a uniform drift velocity throughout all cells conforming a plane. (See Figure 12)

The Y'-plane in chamber 2 shows a significant deviation from the rest. This could indicate a possible variation in the high voltage applied to the field wires in that plane which leads to variations in the electric field causing variations in

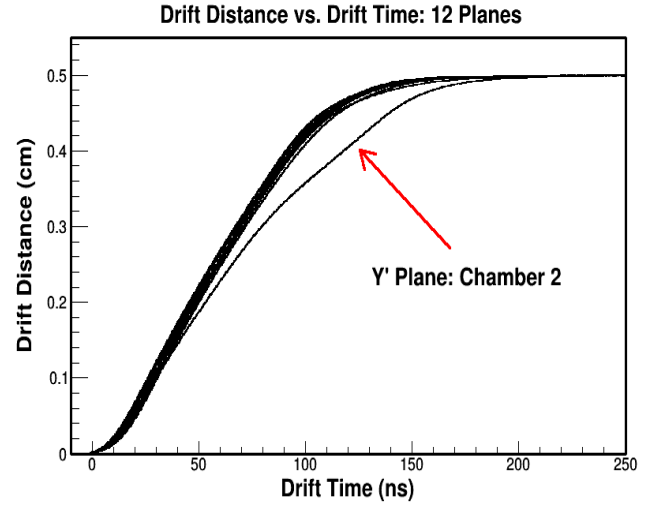
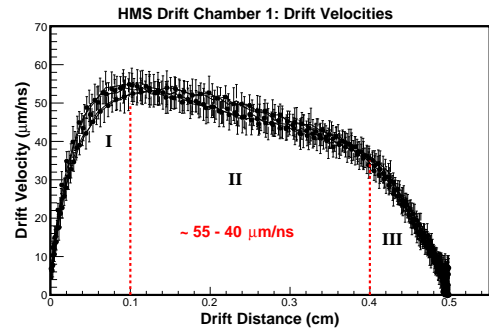
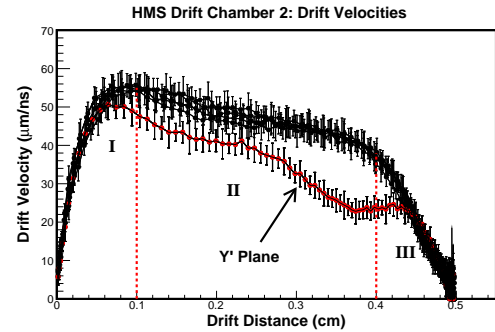


Fig. 12: Correlation between drift distance and drift time for both drift chambers.

drift velocities. (See Figures 13a and 13b)



(a) Drift velocity vs. drift distance for all planes in chamber 1.



(b) Drift velocity vs. drift distance for all planes in chamber 2.

Fig. 13: Drift velocity variation as a function of drift distance for all planes in both chambers.

The linear correlation that exists between drift time and distance in Figure 12 shows the drift velocity is mostly constant throughout all planes. The small variations of drift velocity with drift distance observed in Figure 13, however, shows that the drift velocity is not truly a constant, but varies by a few microns/ns far from the cell edges or center (region II). By performing a linear fit to the time to distance correlation in steps of 2 ns intervals, the small variations in drift velocity become apparent. The slope of the linear fit (drift velocity) was plotted versus the drift distance as shown in Figure 13. From Figure 13, large variations in the drift velocity can also



be observed at the edges (region III) and center (region I) of a cell. This effect is due to the non-uniformity of the electric field in these regions.

## V. DRIFT CHAMBER EFFICIENCIES AND RESIDUALS

The per plane efficiencies were determined for all planes. The efficiency of any given plane in a chamber is defined as the ratio of the number of hits that were detected by the plane to the number of hits that *should* have been detected by that plane. Where a *hit* is defined as a detectable signal in the chamber from ionized charges produced by the passage of a particle. Mathematically, the efficiency of the  $i^{th}$  plane is given by

$$\epsilon_i = \frac{\# \text{ hits that were detected by the } i^{th} \text{ plane}}{\# \text{ hits that should have been detected by the } i^{th} \text{ plane}}$$

with the condition that the hit was also detected by the remaining five planes in the chamber. The efficiencies of both chambers are summarized in Table I.

HMS Drift Chamber Efficiencies		
Plane	Chamber 1 (%)	Chamber 2 (%)
X	95.8	99.4
Y	98.7	99.7
U	97.7	96.6
V	96.5	97.7
Y'	99.0	97.7
X'	94.9	97.2

TABLE I: Drift chamber plane efficiencies

The best way to determine the drift chamber performance is by measuring the spatial resolution, or how well it can measure the position of particle tracks. This measurement is done through the determination of per plane residuals. For a particle traversing at least 4 planes of the chamber, a collection of space-points (X,Y) is measured based on the wires that fired. The space points are fitted with a straight line such as to minimize the chi-square, and obtain a best fit. The line fit is then compared to the measured space-point from the plane wires that fired, and the difference is called the *residual* for that plane. The residuals are calculated on an event by event basis, and should be centered around zero. (See Figure 14)

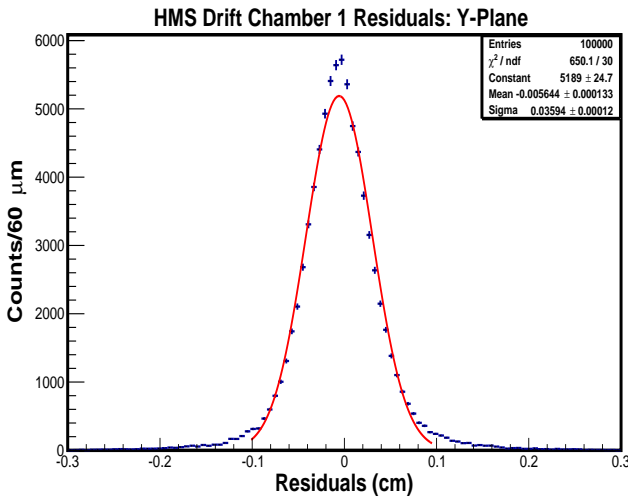


Fig. 14: Residuals for the Y-plane in chamber 1. The Full Width at Half Maximum (FWHM or  $\sigma$ ) is representative the spatial resolution.

A gaussian fit was done for all planes in both chambers to extract the space resolution of the chambers. The fit results are summarized in Table II

HMS Drift Chamber Residuals		
Plane	Chamber 1, $\sigma(\mu m)$	Chamber 2, $\sigma(\mu m)$
X	416 $\pm$ 1.69	388 $\pm$ 1.60
Y	360 $\pm$ 1.18	408 $\pm$ 1.22
U	361 $\pm$ 1.29	327 $\pm$ 1.27
V	382 $\pm$ 1.47	323 $\pm$ 1.28
Y'	383 $\pm$ 1.31	391 $\pm$ 1.16
X'	419 $\pm$ 1.63	384 $\pm$ 1.55

TABLE II: Drift chamber plane residuals

The residuals determined in Table II include contributions from the residuals of the other five planes in each chamber [2]. From fitted curve in Figure 14, the resolutions of the remaining five planes were added in quadrature. In general, the resolution of the  $i^{th}$  plane in each chamber can determined by the following equation

$$\sigma_i^2 = \sigma_1^2 + \sigma_2^2 + \sigma_3^2 + \sigma_4^2 + \sigma_5^2 = 5\sigma^2 \quad (5)$$

since it was assumed that the other five planes have equal contributions to the residual of the sixth plane. The per plane residuals can then be determined by dividing the residual determined from the fit ( $\sigma_i^2$ ) by 5, and taking the square root. For example, the intrinsic resolution of the V-plane in chamber 1 would be  $\sigma_V = 170.8 \pm 0.657 \mu m$ . The intrinsic resolutions per plane are summarized in Table III.

HMS Drift Chamber Intrinsic Resolutions		
Plane	Chamber 1, $\sigma(\mu m)$	Chamber 2, $\sigma(\mu m)$
X	186 $\pm$ 0.755	173.5 $\pm$ 0.715
Y	160.9 $\pm$ 0.527	182.4 $\pm$ 0.545
U	161.4 $\pm$ 0.576	146.2 $\pm$ 0.567
V	170.8 $\pm$ 0.657	144.4 $\pm$ 0.572
Y'	171.2 $\pm$ 0.585	174.8 $\pm$ 0.518
X'	187.3 $\pm$ 0.728	171.7 $\pm$ 0.693

TABLE III: Drift chamber intrinsic spatial resolutions per plane.

## VI. SUMMARY

This report has outlined the steps taken to calibrate the HMS drift chambers using data taken on March 2017. The outline also covered some of the difficulties encountered in the calibration procedure, and the steps taken to overcome them. The effects of the gas mixture and applied high voltage on the drift velocities was also briefly discussed. Finally, two performance criterions (efficiencies and residuals) used to describe the performance of the drift chambers were investigated. The efficiencies described how well were the chambers able to detect hits produced by the passage of a particle. The residuals described how well does the measured particle position in each plane compare to the best track fit through all six planes in each chamber.

## REFERENCES

- [1] MEEKINS, D. G. *Coherent  $\pi^0$  Photoproduction on the Deuteron*. PhD thesis, Williamsburg, VA, 1998.
- [2] O.K. BAKER, E. A. The High Momentum Spectrometer drift chambers in Hall C at CEBAF. *Nuclear Instruments and Methods in Physics Research A*, 367 (1995), 92–95.